Step Climbing and Descending for a Manual Wheelchair with a Network Care Robot

Hidetoshi Ikeda, Hikaru Kanda and Nobuyuki Yamashima
Department of Mechanical Engineering
Toyama National College of Technology (Hongou campus)
13 Hongou-chou, Toyama-shi, Japan
E-mail: ikedah@nc-toyama.ac.jp

Eiji Nakano
Robofesta Org.
Narashino-shi, Japan
E-mail: nakanoeini@gmail.com

***Abstract*—Realization of step climbing or descending for a heavy cart or a wheelchair using human-friendly robot with manipulators is a technical issue. This paper describes cooperative step climbing and descending tactics for a manual wheelchair and a partner robot that is equipped with manipulators driven by small direct current motors. When the wheelchair and robot climb or descend a step, these vehicles are linked together by the robot hands, and some of the manipulator joints are allowed to move passively. Thus, the manipulators motors do not need to exert major torque to support the vehicles. The velocity differences between the two vehicles is used to pass over the step. When the wheelchair is climbing or descending, the upper links of the manipulators are pressed against the robot's chest to stabilize the wheelchair's movements. In addition, the forearm links of the robot are pressed against, or fixed to, the back of the wheelchair. The robot equipped with manipulators driven by small motors allows the wheelchair to overcome a step, and then the robot itself is able to overcome the step by using the wheelchair. In an experiment, we connected a teleoperation system for the robot through an intranet and confirmed that these vehicles could cooperatively climb and descend steps.**

Keywords—step climbing; wheelchair; robot; cooperation

I. INTRODUCTION

Without a human assistant, most wheelchair users are not able to enter an area that has steps. Thus, they need a special wheelchair equipped with a step climbing or descending mechanism. Wheelchairs with such special mechanisms have been widely researched and include, for example, a wheelchair with additional legs [1], a wheelchair with multiple wheels [2] [3], a wheelchair with multiple wheels connected by active linkages [4], a wheelchair with an adjustable center of gravity [5], a wheelchair with a combination of an adjustable center of gravity and multiple wheels [6], a wheelchair with special wheels [7], and a tracked vehicle [8]. These mechanisms can provide the wheelchair with the ability to climb stairs or surmount other obstacles. The research group of the present report achieved cooperative step climbing of a wheelchair connected to a wheeled robot by passive links [9] and, separately, of a wheelchair and a wheeled robot with manipulators [10]. This report presents the step climbing and descending method for a wheelchair and a care robot having dual manipulators that allow the wheelchair user to overcome many of the obstacles encountered in daily life. Because most of the human-friendly robots that are used in homes or offices have small motors due to their limited body size, it is difficult for such robots to lift heavy vehicles. In addition, precisely controlling the axes' angles of the manipulators according to the processes related to pushing and pulling, and in relation to the vehicle's incline is very difficult. In such cases slippage of driving wheels can occur or the vehicles can tip over. Thus, mobile robots with manipulators have not previously been used to assist heavy carts or wheelchairs in step climbing and descending. In the method used in this study, some of manipulator joints and the upper links or forearm links of manipulators press passively against the robot or wheelchair when these vehicles climb or descend a step. Thus, the motors do not need to exert major torque to support with vehicles.

The wheelchair users considered in the present study were assumed to have the upper-body capability of an able-bodied person. Based on preliminary measurements, the friction coefficients of the vehicles and the ground surface in this research were assumed to be in the range of 0.6 to 0.9, and the target step height was set at a maximum of 0.12 [m] (More than 80% of the observed step heights were lower than 0.12 [m]) .

This paper is organized as follows. Section II describes the cooperative step-climbing system and Section III describes the step climbing and descending procedures. Section IV provides the theoretical analysis. Section V describes an experiment and presents the experimental results, and Section VI is the conclusion.

II. ROBOT AND WHEELCHAIR

The robot used in this research is the wheeled "Tateyama" developed in this laboratory (Figure 1). TABLE I lists the specifications. When passing over a step, the wheelchair and robot are deployed in a forward-and-aft configuration (Figure 2). This robot has three sets of wheels consisting of front, middle, and rear pairs on the left and right sides. The front and rear pairs are casters whose positions can be shifted, while the middle pair are the driving wheels. The robot has manipulators attached to the left and right sides of its upper half: each arm has 5 degrees of freedom (DOF) and each hand has 1 DOF for a total of 6 DOF (Figs. 1 and 3). In this study, the length from Joint 2 (shoulder) to Joint 4 (elbow) is called "Link 2" (length l_2), from Joint 4 (elbow) to Joint 5 (wrist) is called "Link 4" (length l_4), and from Joint 5 (wrist) to the tip of the hand is called "Link 6" (length l_6). The length from Joint 4 (elbow) to Joint 6 (the location of the connection between the wheelchair and the robot) is designated l_{4C}. The manipulator joint angles are -90 [deg] $\leq \phi_2 \leq$ +90 [deg] and 0 [deg] $\leq \phi_4 \leq$ +100

 ISBN: 978-1-61208-269-1

TABLE I. ROBOT SPECIFICATIONS.

Overall length	0.230–0.800 [m]
Overall height	0.747 [m]
Radius of front wheels (r_{Bf})	0.025 [m]
Radius of middle wheels (R_B)	0.145 [m]
Radius of rear wheels (r_{Br})	0.019 [m]
Wheelbase (WB_f)	0.190–0.440 [m]
Wheelbase (WB_r)	0.270 [m]
Mass position from the rear axes (l_{rB})	0.093 [m]
Height of the mass from the rear axes (h_{mB})	0.286 [m]
Position of Joint 2 from the rear axes (l_{LB})	0.090 [m]
Height of Joint 2 from the rear axes (h_{LB})	0.532 [m]
Mass of the robot body	55 [kg]
Mass of link 2 (from Joints 2 to 4)	2.55 ×2 [kg]
Mass of link 4 (from Joint 4 to hand)	0.8 ×2 [kg]
Length of link 2 (l_2)	0.330 [m]
Length of link 4 (l_4)	0.300 [m]
Length of the hand (l_6)	0.105 [m]
Length from Joint 4 to the connecting position (l_{4c})	0.370 [m]
Mass position of link 2 (L_2)	0.067 [m]
Mass position of link 4 (L_4)	0.169 [m]
Mass position of link 6 (hand mechanism) (L_6)	0.035 [m]

TABLE II. SPECIFICATIONS OF THE MANUAL WHEELCHAIR.

Overall length	1.060 [m]
Overall height	0.985 [m]
Radius of front wheels (r_A)	0.063 [m]
Radius of rear wheels (R_A)	0.300 [m]
Wheelbase (l_A)	0.430 [m]
Handrim position (l_{LA})	0.250 [m]
Mass position from the rear wheel axes (l_{rA})	0.149 [m]
Height of mass from rear wheel axes (h_{mA})	0.371 [m]
Mass (wheelchair + driver) (M_A)	92.7 [kg]

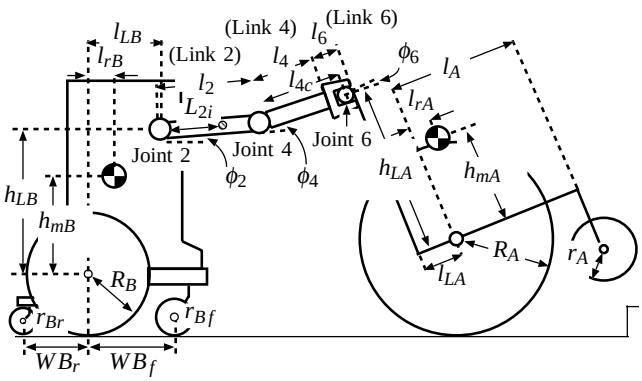

Figure 2. Model of the wheelchair and robot.

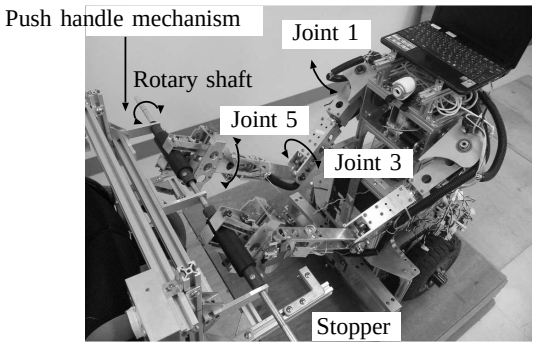

Figure 3. Push handle mechanism of the wheelchair.

[deg]. The hands consist of two fingers that open and close in order to grasp items (Figure 3). These axes and the hands are driven by small direct current (DC) motors (Joints 1, 2: 20 [W], Joints 3, 4: 6 [W], Joint 5: 2.5 [W], 1.5 [W]). The robot also has a stopper mounted on the front part of its body (Figs. 4 (a) and 5 (a)). The stopper limits the passive rotational travel of the robot manipulators and thus enables the robot to imitate the operation of a human pushing an object by limiting the passive rotation about the shoulder joint as the upper arm is pushed into the chest of the robot when the wheelchair climbs (Figure 5 (a)) and descends a step (Figure 5 (b)).

The wheelchair (NOVA Integral-ME) has a shape typical of wheelchairs currently available in the market (Figure 1). TABLE II provides the specifications. This is a manually operated chair to which an electric drive unit was added. In this study, the wheelchair is operated manually by the user, but it is also equipped a push handle mechanism on the back that is held by the robot hands (Figure 3). This system needs 2.07 [m] step length. The push handle mechanism is composed of a rotary shaft that allows passive rotation and a stopper for use when the robot is climbing or descending. The hand mechanism grasps the shaft to connect the two vehicles. The angle ϕ_6 is formed by the wheelchair with Link 4 (Figure 2). The stopper of the wheelchair is composed of front and rear bars (Figs. 6 (a) and (b)), and is mounted on the rear side. When the robot is climbing or descending, the sides of the robot are opened, and the two manipulators are inserted into the stopper (Figure 6 (a)). The robot pushes the front bars to lift its front wheels (Figure 6 (a)). The rear bars are used to prevent it from tipping over backward when the robot's mass position shifts behind the contact point between the center wheels and the ground (Figure 6 (b)).

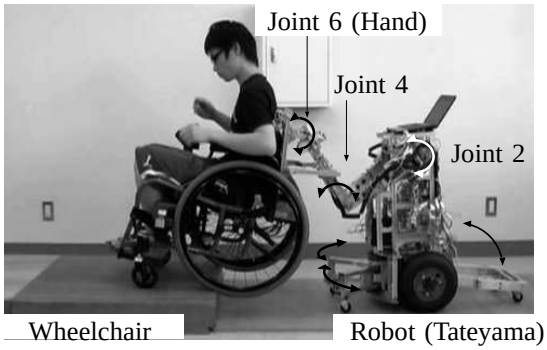

Figure 1. The wheelchair and the robot.

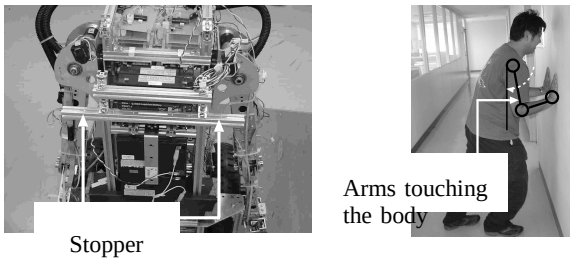

Figure 4. Control of rotary motions of the robot shoulder is performed by using the body. (a) The front body of the robot. (b) A human pushing an object.

 ISBN: 978-1-61208-269-1

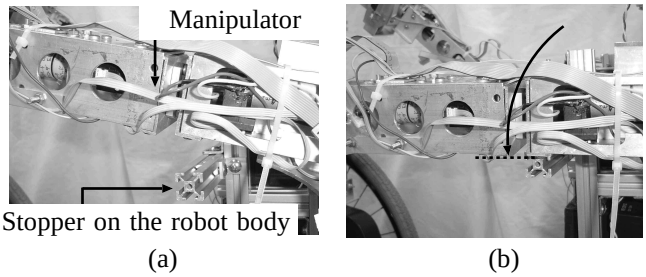

Figure 5. Stopper details. (a) Pulling the wheelchair. (b) Pushing the wheelchair.

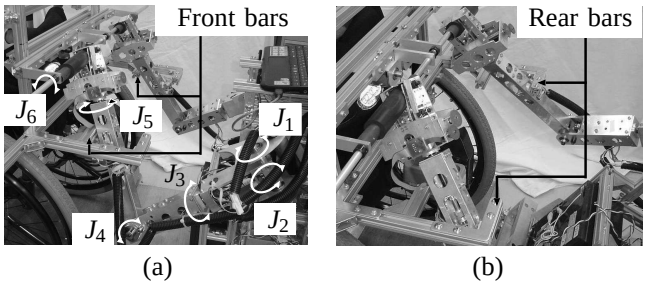

Figure 6. Action of the stopper. (a) Lifting the wheels of the robot. (b) Preventing the robot from falling down.

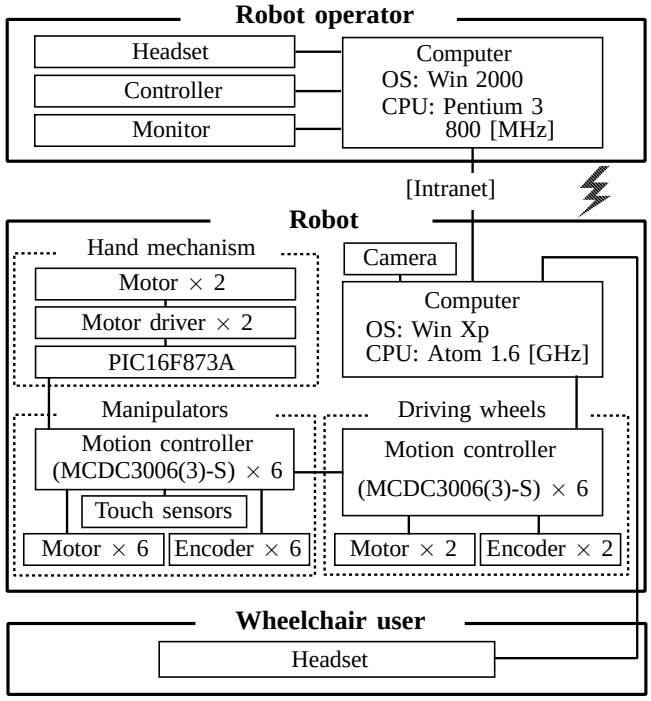

Figure 7. Diagram of the robot system.

Figure 7 is a diagram of the system configuration. The motors mounted on the robot are connected to Faulhaber motion controllers (Faulhaber MCDC3006-S, MCDC3003-S). In turn, these are connected to a notebook PC mounted on the robot. The motors are controlled via commands issued using the Faulhaber Motion Manager 4 software package. The robot employs a camera built into the PC, and the moving images from that camera and the Motion Manager 4 operating window are displayed on the notebook PC mounted on the robot. This notebook PC uses RealVNC remote access and control software and data is transmitted over the intranet as-is to the display of the PC used by the caregiver in a different location. The caregiver and the wheelchair user both wear headsets and use Skype telecommunication software to communicate verbally. The caregiver's headset is connected to the caregiver's PC, and the wheelchair user's headset is connected to the PC on the robot. The caregiver controls the robot by operating Motion Manager 4 from his PC. The keyboard commands for Motion Manager 4, which are issued using JoyToKey software, correspond to the manipulation by the caregiver to operate the robot. The robot has internal and external sensors (encoders and touch sensors). Thus, the robot is moved by the information integrated in the sensors' signals with the commands from the caregiver.

III. Process of Moving over a Step

When encountering a step, the robot hands grasp the rotary shaft of the wheelchair push handle mechanism, thus linking itself to the wheelchair. The chair is then controlled to raise first its front wheels, and then its back wheels, onto the upper level of the step. The ascent and descent processes are described below. The stages shown in Figs. 8–11 correspond to (1)–(32) below; "Forward" or "Backward" and signifies the robot or the wheelchair's motion ahead or behind, respectively. "Free" is the state in which the vehicle does not do anything. "Stop" is the state in which the vehicle does not move.

[Stage 1]

(1) The robot hand grasps the wheelchair push handle to link the two vehicles. Joints 2, 4, and 6 are allowed to rotate passively until the ascent of the wheelchair has been completed. (2) The robot controller stops the robot. The wheelchair user manipulates the handrims as if to move forward, lifting the front wheels. (3) As the wheelchair tilt increases, if the location of the wheelchair's center of mass shifts behind the contact point between the back wheels and the ground, the chair exerts forces on the manipulators, causing passive rotation about Joint 2 (Figure 5 (b)). In this case, the bottom part of the manipulator upper-arm link comes into contact with the stopper and limits the extent of the rotation (Figure 5 (b)). Thus, the robot supports the wheelchair from behind to prevent the wheelchair from tipping over backward. (4) The robot moves forward and the wheelchair user manipulates the handrims to adjust the difference between the speeds of the two vehicles, so that the front wheels of the wheelchair are placed on the upper level of the step. After completion of stage 1, the wheelchair user does not perform any operations until the end of stage 2.

[Stage 2]

(5) The robot continues to move forward while pushing the wheelchair from behind. (6) The back wheels of the wheelchair then come into contact with the step. (7) The robot continues to push on the wheelchair so that the rear wheels of the wheelchair climb up onto the step. The robot supports the wheelchair during this process to prevent the wheelchair from tipping over backward. (8) Once the wheelchair rear wheels have reached the upper level of the step, the robot stops.

 ISBN: 978-1-61208-269-1

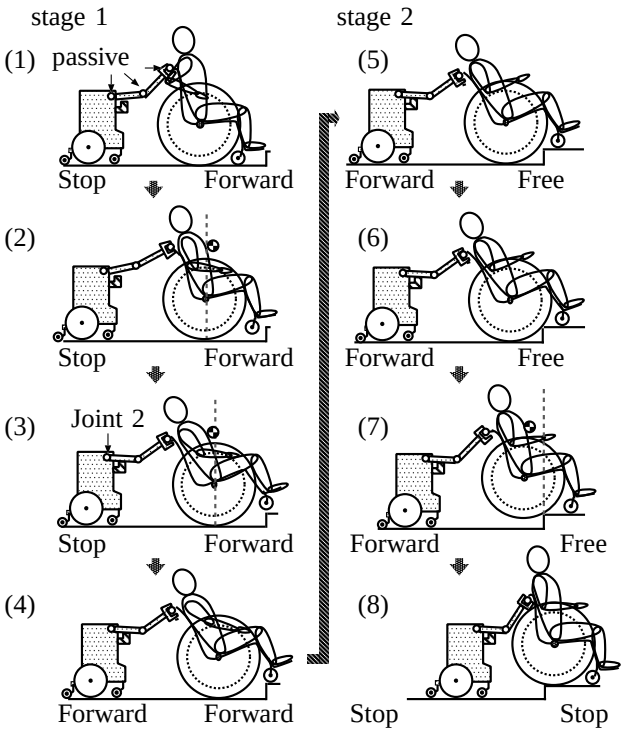

Figure 8. Step-climbing process of the wheelchair (stages 1, 2).

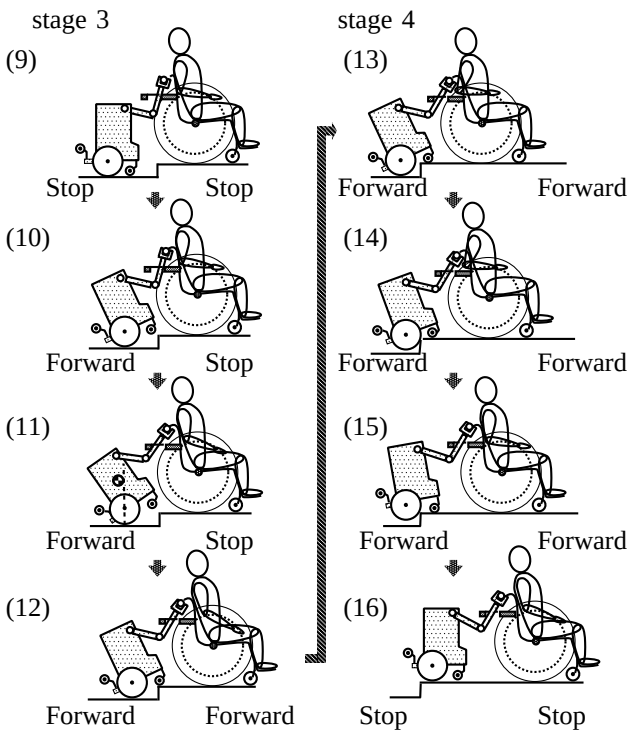

Figure 9. Step-climbing process of the robot (stages 3, 4).

[Stage 3]

(9) After stage 2, the rear wheels of the robot are folded upward. The sides of the robot are opened, and the two manipulators are inserted into the stopper (Figure 6 (a)). The wheelchair user holds the handrims and maintains the position of the wheelchair. The robot moves forward, the manipulator forearm link comes into contact with the stopper of the wheelchair (Figure 6 (a)). (10) The robot continues to push on the wheelchair and the front wheels of the robot are lifted. (11) As the robot tilt increases, if the location of the center of mass of the robot shifts behind the contact point between its middle wheels and the ground, the robot begins to tip over backward, but part of the manipulator forearm link comes into contact with the stopper of the wheelchair and limits the extent of rotation (Figure 6 (b)). Thus, the wheelchair supports the robot and prevents it from tipping over backward. (12) The robot then moves forward and the wheelchair user manipulates the handrims, thereby adjusting the difference between the speeds of the two vehicles so that the front wheels of the robot are placed on the upper level of the step.

[Stage 4]

(13) Both vehicles move forward. (14) The middle wheels of the robot come into contact with the step. The wheelchair pulls the robot, and the value of the normal reaction from the step on the robot middle wheels (driving wheels) is increased. Consequently, the force of the manipulators prevent the robot from falling down. The middle wheels of the robot then start to climb the step. (15) Both vehicles continue to move forward. (16) The center wheels of the robot are able to climb the step. Once the robot middle wheels have reached the upper level of the step, both vehicles are stopped.

[Stage 5]

(17) The robot hand grasps the wheelchair push handle to link the two vehicles. The sides of the robot are opened, and the two manipulators are inserted into the wheelchair stopper (Figure 6 (a)). Joint 1 is fixed. Joints 2 to 6 are allowed to rotate passively until the descent of the robot has been completed. In the robot descending process (stages 5, 6), the front wheels of the robot are closed and the rear wheels are folded upward. Both vehicles move backward. (18) After the rear wheel axes of the robot reach the corner of the step, the robot tilt increases and the robot begins to tip over backward. However, at this stage the forearm link comes into contact with the wheelchair stopper and limits the extent of rotation (Figure 6 (b)). (19) Thus, the wheelchair supports the robot and prevents it from tipping over backward. (20) As a result, the middle wheels of the robot are able to descend the step.

[Stage 6]

(21) Both vehicles continue to move backward. (22) The wheelchair moves faster than the robot, and thus the wheelchair front stopper pushes on the manipulator forearm link. The front wheel axes of the robot reach the corner of the step. (23) The wheelchair stops, and the robot continues to move. (24) As a result, the front wheels of the robot are able to descend the step.

[Stage 7]

(25) In the wheelchair descent process (stages 7, 8), the front wheels of the robot are opened and the rear wheels are lowered. The sides of the robot are closed (Figure 3). Joints 2, 4, and 6 are allowed to rotate passively until the descent of

 ISBN: 978-1-61208-269-1

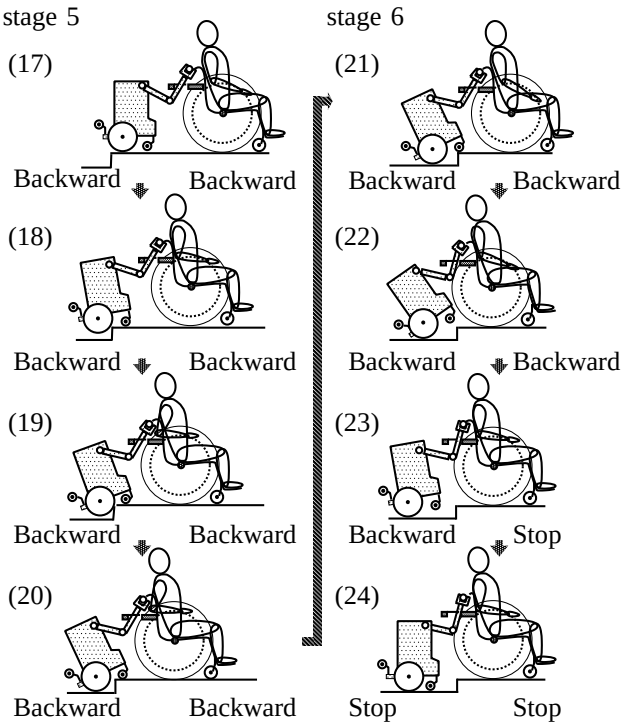

Figure 10. The step descending process (stages 5, 6).

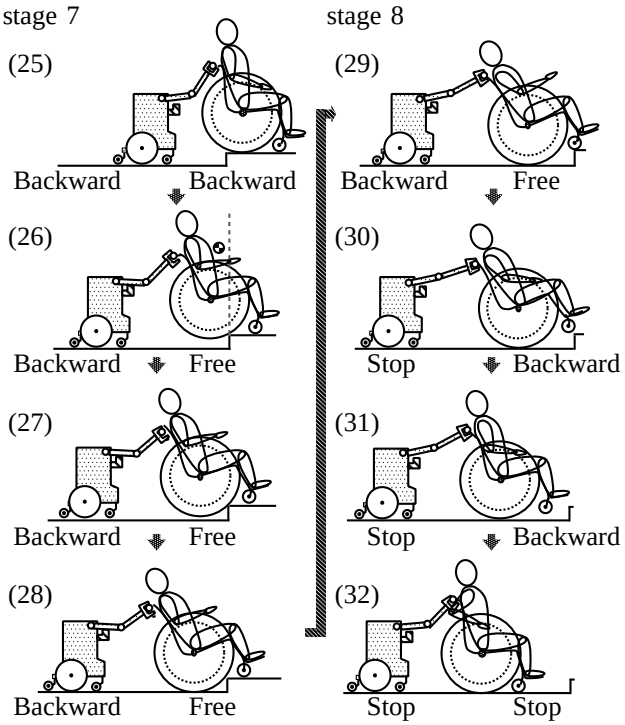

Figure 11. The step descending process (stages 7, 8).

the wheelchair has been completed. (26) As the robot moves backward, the wheelchair user does not perform any operations until the end of stage 7, and the wheelchair is pulled by the robot. The rear wheels of the wheelchair begin to descend the step. (27) The upper arm pushes against the chest (robot stopper) to limit the passive rotation about the shoulder axes. Thus, the robot supports the wheelchair during this process to prevent the wheelchair from tipping over backward. (28) The rear wheels of the wheelchair descend the step.

[Stage 8]

(29) Both vehicles continue to move backward. (30) After the front wheel axes of the wheelchair reach the corner of the step, the wheelchair user manipulates the handrims as if to lift the front wheels. (31) The wheelchair user increases the wheelchair speed with both hands, and the incline of the wheelchair begin to decrease. (32) As a result, the rear wheels of the wheelchair are able to descend the step.

IV. Theoretical Analysis

The requirements of preventing slippage in stage 1 are listed below. Figs. 12, 13 show f_{1x}, f_{2z}, $\cdots$, f_{6z}.

$$(i) \quad \mu > |f_{5x}|/f_{6z} \ (\phi_2+\phi_4+\phi_6 = 0)$$
$$(ii) \quad \mu > |f_{1x}|/f_{2z} \ (\phi_2+\phi_4+\phi_6 = 0)$$
$$(iii) \quad \mu > |f_{5x}|/f_{6z} \ (\phi_2+\phi_4+\phi_6 = 24.54 \text{ [deg]})$$
$$(iv) \quad \mu > |f_{1x}|/f_{2z} \ (\phi_2+\phi_4+\phi_6 = 24.54 \text{ [deg]})$$

(i) and (ii) are the requirements to lift the front wheels of the wheelchair from the ground (Figure 8 (1)–(2)). (iii) and (iv) are the requirements to prevent the wheelchair from tipping over backward (Figure 8 (3)–(4)). Here, 24.54 [deg] is the maximum incline of the wheelchair when the wheelchair operator climbs a step, and the height between the lowest point on the front wheel tread surface and the ground surface below the step is $h_t = 0.200$ [m] (Figure 12). It was observed that people tend to raise the front wheels higher than the step they intend to traverse when actually operating a wheelchair. Thus, h_t was measured for five participants and the results were used when specifying a maximum tilt angle.

Figure 12 shows the stage 1 state in which the wheelchair center of mass is forward of the contact point between the rear wheels and the ground (Figure 8 (1)–(2)). At this time point, the robot is stopped, the wheelchair is propelled, and the robot exerts a backward force by pulling on the wheelchair. Figure 13 shows the state when the tilt of the wheelchair is increasing, and the wheelchair center of mass is behind the contact point between the rear wheel and the ground (Figure 8 (3)–(4)). When the situation shown in Figure 12 changes to that shown in Figure 13, the manipulators rotate passively. In this procedure, the stoppers limit the amount of passive rotation about the robot shoulder joint (Figure 5 (b)).

Σ_B is the basic coordinate system for the robot, where contact point B is between the robot middle (driving) wheels and the ground is the origin (Figure 13). Joints 2 (shoulder), 4 (elbow), and 6 (location where the hands hold the push handle) are controlled passively. The position vectors for these joints in system Σ_B are expressed as ${}^B\boldsymbol{p}_{2i} = [x_{2i} \ z_{2i}]^T$ ($i = 1 \sim 3$), where ${}^B\boldsymbol{p}_2 = [x_2 \ z_2]^T = [l_{LB} \quad R_B + h_{LB}]^T$, ${}^B\boldsymbol{p}_4 = [x_4 \ z_4]^T = [l_{LB} + l_2\cos\phi_2 \quad R_B + h_{LB} + l_2\sin\phi_2]^T$, and ${}^B\boldsymbol{p}_6 = [x_6 \ z_6]^T = [l_{LB} + l_2\cos\phi_2 + l_{4c}\cos(\phi_2+\phi_4) \quad R_B + h_{LB} + l_2\sin\phi_2 + l_{4c}\sin(\phi_2+\phi_4)]^T$ (Figure 2).

In the same way, the position vectors for the contact points between the robot front and rear wheels and the ground are

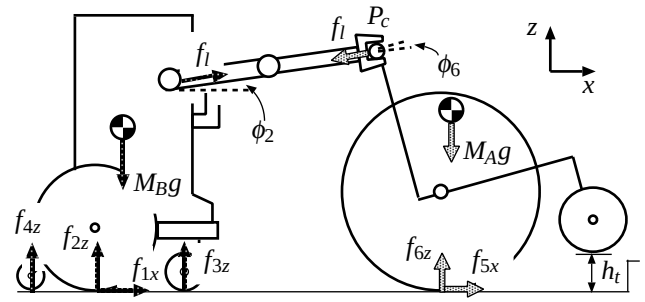

Figure 12. The step-climbing system using the wheelchair and the wheeled robot.

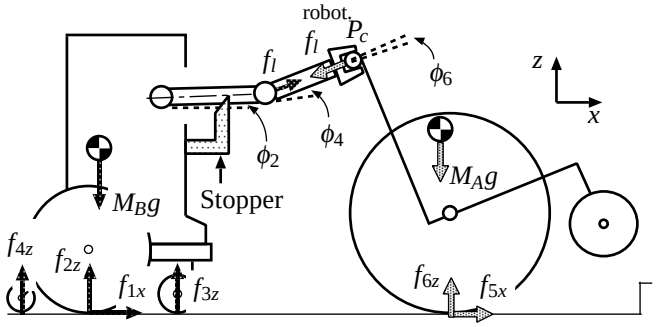

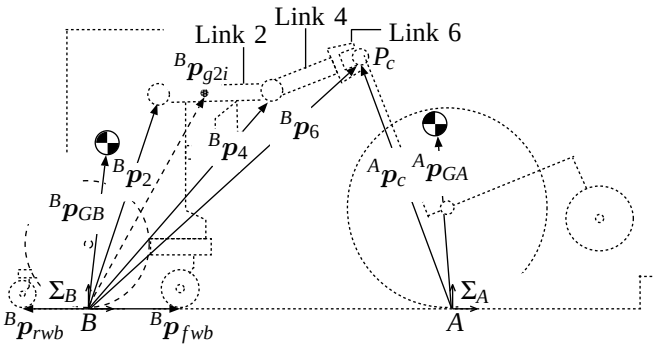

Figure 13. Step-climbing system using the wheelchair and the wheeled robot.

expressed as ${}^B\boldsymbol{p}_{fwb} = [WB_f \;\; 0]^T$ and ${}^B\boldsymbol{p}_{rwB} = [-WB_r \;\; 0]^T$, respectively. The body of the robot, neglecting the manipulators, is Link 0 with mass m_0. If the centers of mass of the robot body and each manipulator link (Links 2, 4, and 6) are denoted by ${}^B\boldsymbol{p}_{gj} = [x_{g2j} \;\; z_{g2j}]^T$ (where j = 0–3), then the center of mass of the entire robot ${}^B\boldsymbol{p}_{GB} = [x_{GB} \;\; z_{GB}]^T$ is given by ${}^B\boldsymbol{p}_{GB} = (\Sigma_{j=0}^3 m_{2j}^B \boldsymbol{p}_{g2j})/\Sigma_{j=0}^3 m_{2j}$. The driving force vector for the robot middle wheels is $\boldsymbol{f}_1 = [f_{1x} \;\; 0]^T$, and the resistance force from the ground surface is $\boldsymbol{f}_2 = [0 \;\; f_{2z}]^T$. Additionally, the resistance force at the robot front wheels is $\boldsymbol{f}_3 = [0 \;\; f_{3z}]^T$, and that at the rear wheels is $\boldsymbol{f}_4 = [0 \;\; f_{4z}]^T$. The reaction force from the linked wheelchair is given by $\boldsymbol{f}_{\boldsymbol{L}} = [f_l \cos(\phi_2+\phi_4) \quad f_l \sin(\phi_2+\phi_4)]^T$. Σ_A for the wheelchair is the coordinate system fixed at the point of contact between the wheelchair rear wheels and the ground, A. In Σ_A, the wheelchair center of mass is located at ${}^A\boldsymbol{p}_{GA} = [x_{GA} \;\; z_{GA}]^T = [l_r \cos(\phi_2+\phi_4+\phi_6) - h_m \sin(\phi_2+\phi_4+\phi_6) \quad l_r \sin(\phi_2+\phi_4+\phi_6) + h_m \cos(\phi_2+\phi_4+\phi_6) + R_A]^T$, and the push handle location (where it is held by the robot hand) P_c is ${}^A\boldsymbol{p}_c = [x_c \;\; z_c]^T = [-l_{LA}\cos(\phi_2+\phi_4+\phi_6) - h_{LA}\sin(\phi_2+\phi_4+\phi_6) \quad -l_{LA}\sin(\phi_2+\phi_4+\phi_6) + h_{LA}\cos(\phi_2+\phi_4+\phi_6) + R_A]^T$.

The driving force at the wheelchair rear wheels is $\boldsymbol{f}_5 = [f_{5x} \;\; 0]^T$, and the resistance force felt at the ground surface is $\boldsymbol{f}_6 = [0 \;\; f_{6z}]^T$. Furthermore, the reaction force from the linked robot is given by $\boldsymbol{f}'_{\boldsymbol{L}} = [-f_l \cos(\phi_2+\phi_4) \quad -f_l \sin(\phi_2+\phi_4)]^T$.

Summing the total forces on the wheelchair exerted by the ground surface (resistance) and by the linked robot for $\boldsymbol{f}_{\Sigma A} \in \boldsymbol{R}^2$, we find that $\boldsymbol{f}_{\Sigma A} = [f_{5x} - f_l \cos(\phi_2+\phi_4) \quad f_{6z} - f_l \sin(\phi_2+\phi_4)]^T$. When the linked vehicles are moving together in static equilibrium, the equilibrium for both the x and z axes yields (1), while the equilibrium of moments about the point of contact between the wheelchair rear wheels and the ground yields (2). Here, $\boldsymbol{g} = [0 \;\; -g]^T$ is gravitational acceleration.

$$\boldsymbol{f}_{\Sigma A} + \mathrm{M}_A \boldsymbol{g} = 0 \tag{1}$$

$${}^A\boldsymbol{p}_{GA} \times \mathrm{M}_A \boldsymbol{g} + {}^A\boldsymbol{p}_c \times \boldsymbol{f}'_{\boldsymbol{L}} = 0 \tag{2}$$

We obtain (3) and (4) from (1).

$$f_{5x} = f_l \cos(\phi_2+\phi_4) \tag{3}$$

$$f_{6z} = M_A g + f_l \sin(\phi_2+\phi_4) \tag{4}$$

Then, from (2), we find

$$f_l = \frac{x_{GA} M_A g}{z_c \cos(\phi_2+\phi_4) - x_c \sin(\phi_2+\phi_4)} \tag{5}$$

Next, from the z-coordinate of ${}^B\boldsymbol{p}_6$ and ${}^A\boldsymbol{p}_c$, we obtain

$$h_{LA} = \frac{z_6 + l_{LA}\sin(\phi_2+\phi_4+\phi_6) - R_A}{\cos(\phi_2+\phi_4+\phi_6)} \tag{6}$$

where $z_6 = R_B + h_{LB} + l_2 \sin\phi_2 + l_{4c}\sin(\phi_2+\phi_4))$. When the robot acts statically in stage 1, (7) holds, and the equilibrium in the x and z axes gives us

$$\boldsymbol{f}_{\Sigma B} + M_B \boldsymbol{g} = 0 \tag{7}$$

Here, $\boldsymbol{f}_{\Sigma B} \in \boldsymbol{R}^2$ is the sum of forces on the robot due to resistance at the ground surface and from the linked wheelchair, and $\boldsymbol{f}_{\Sigma B} = [f_{1x} + f_l \cos(\phi_2+\phi_4) \quad \Sigma_{k=2}^4 f_{kz} + f_l \sin(\phi_2+\phi_4)]^T$.

From (7), we obtain (8) and (9).

$$f_{1x} = -f_l \cos(\phi_2+\phi_4) \tag{8}$$

$$f_{2z} = M_B g - f_l \sin(\phi_2+\phi_4) - f_{3z} - f_{4z} \tag{9}$$

During the process of moving over a step, while the manipulators are pulling the robot wheelchair (Figure 12), the manipulators and stoppers do not come into contact. By the equilibrium of moments about the contact point between the robot driving wheel and the ground during this time, we obtain

$${}^B\boldsymbol{p}_{GB} \times \mathrm{M}_B \boldsymbol{g} + {}^B\boldsymbol{p}_2 \times \boldsymbol{f}_{\boldsymbol{L}} + {}^B\boldsymbol{p}_{fwB} \times \boldsymbol{f}_3 + {}^B\boldsymbol{p}_{rwB} \times \boldsymbol{f}_4 = 0 \tag{10}$$

from which is obtained

$$x_{GB} M_B g - f_l\{x_2 \sin(\phi_2+\phi_4) - z_2 \cos(\phi_2+\phi_4)\} + WB_r f_{4z} - WB_f f_{3z} = 0 \tag{11}$$

When the robot is supporting the wheelchair from behind (Figure 13), passive rotation about Joint 2 (shoulder) is limited by the stopper. At such times, Link 2 (the upper arm of the manipulator) can be treated as a part of the robot body and the equilibrium of moments about the contact point between the robot driving wheels is represented as

$${}^B\boldsymbol{p}_{GB} \times \mathrm{M}_B \boldsymbol{g} + {}^B\boldsymbol{p}_4 \times \boldsymbol{f}_{\boldsymbol{L}} + {}^B\boldsymbol{p}_{fwB} \times \boldsymbol{f}_3 + {}^B\boldsymbol{p}_{rwB} \times \boldsymbol{f}_4 = 0 \tag{12}$$

 ISBN: 978-1-61208-269-1

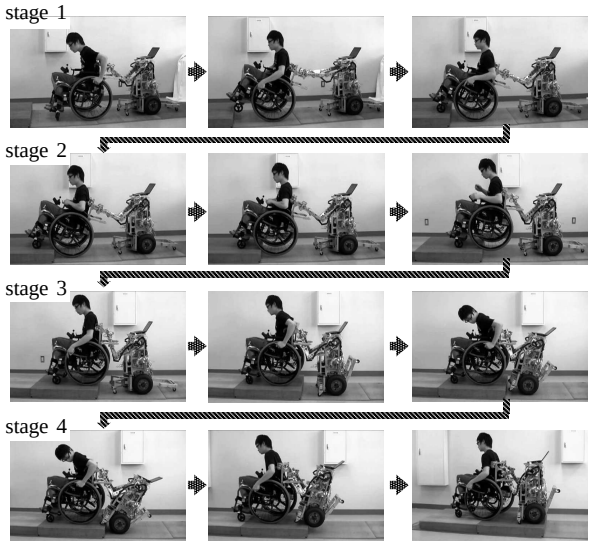

Figure 14. Experiment (Step climbing)

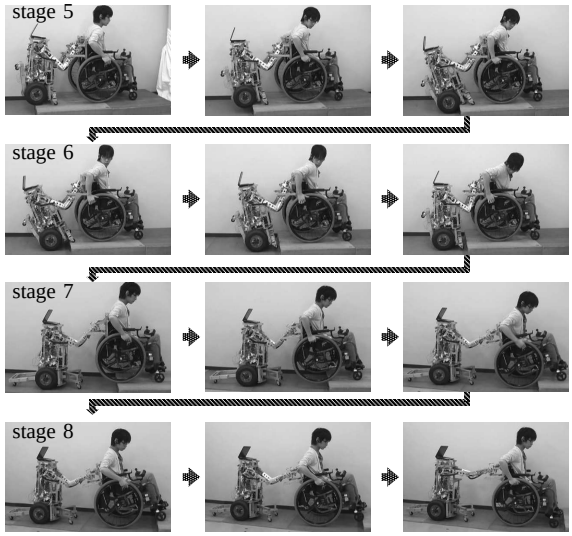

Figure 15. Experiment (Step descending)

from which is obtained

$$x_{GB}M_Bg - f_l\{x_4\sin(\phi_2+\phi_4) - z_4\cos(\phi_2+\phi_4)\} + WB_r f_{4z} - WB_f f_{3z} = 0 \quad (13)$$

We obtain f_{3z} and f_{4z} from (10) and (12). In addition, $\mu > |f_{1x}|/f_{2z}$ or $\mu > |f_{5x}|/f_{6z}$ can be calculated from (3)–(6), (8), and (9).

V. Experiment

An experiment was carried out using this system under an environment of step height 0.12 [m] and friction coefficient $\mu = 0.72$ (Figure 14). The wheelchair user and robot operator were both able-bodied adult males. The wheelchair user and the robot were placed on one floor of the Toyama National College of Technology, and the robot operator was on another floor of the same building. The robot operator performed his task over the intranet while observing the situation via a camera and communicating with the wheelchair user over a voice link.

If the wheelchair was too close to the step in stage 1, the front wheels bumped into the vertical riser of the step. However, following instructions from the wheelchair user, the robot controller was able to back up the two linked vehicles together and re-start the ascent. It was then possible for the front wheels of the wheelchair to climb the step with ease.

Subsequently, during stage 2, the user never needed to push the wheels. More specifically, it was possible to lift the chair onto the upper level of the step by following the procedure proposed above and using only the forward operation of the robot. Stages 3 and 4 were then executed.

Stages 5–8 were performed similarly. In these processes, the wheelchair user twisted his upper body to visually verify the position of the step behind the wheelchair. It should be noted that this system is intended for wheelchair users who can freely move their upper bodies, and one can anticipate that this movement and posture would be difficult for users with certain physical limitations.

In the climbing or descending processes, both vehicles incline in turn. However, because this system only has one camera installed on the robot, the visual information provided was limited and the robot operator experienced some difficulty controlling the robot. Thus, it is clear that the construction of a system to support the robot operator and the wheelchair operator based on exterior and perhaps other sensors would be required in the future.

VI. Conclusion

This report describes the tactics of cooperative step climbing and descending for a manual wheelchair using a robot that imitates the motion of the upper arms of a human pushing his/her chest against a heavy object to move it. We constructed the robot system and an experiment was carried out that incorporated teleoperation of the robot over an intranet. The effectiveness of the handling method for a heavy object was demonstrated by using a robot with manipulators driven by small motors. During the climbing or descending processes, these vehicles incline in turn. However, because this system only has one camera installed on the robot, the visual information supplied to the robot operator was limited. Thus, it is clear that the robot operator will need an enhanced support system that can indicate the distance from the step and show other situations related to the vehicle. It is also clear that the construction of a system to support the wheelchair operator based on exterior and perhaps other sensors would be required in the future.

Despite the above observation, it is worthwhile to demonstrate that mobile manipulators, which are driven by the small motors, are capable of handling a heavy cart (wheelchair) by the method of pressing the manipulator links against the vehicles in addition to the robot hands. In the future, we will verify the force necessary to operate the wheelchair using

 ISBN: 978-1-61208-269-1

this method and an autonomous control system to assist the wheelchair user and robot operator will be built.

ACKNOWLEDGMENT

This work was supported in part by a grant from the Daiwa Securities Health Foundation (2007, Grant No. 19) and the Okawa Foundation for Information and Telecommunications (2008, Grant No. 08-18).

REFERENCES

[1] V. Kumar and V. Krovi, "Optimal traction control in a wheelchair with legs and wheels," Proc. of 4th National Applied Mechanisms and Robotics Conference, December 1995, pp. 95-030-01–95-030-07.

[2] N. Yanagihara, F. Sugasawa, N. Suzuki, T. Ikeda, and Y. Kanaumi, "Mechanical analysis of a stair-climbing wheelchair using rotary cross arm with wheels," Proc. 17th Annual Conference of the Robotics Society of Japan, September 1999, pp. 1143–1144.

[3] G. Quaglia, W. Franco, and R. Oderio, "Wheelchair.q motorized wheelchair with stair climbing ability," Mechanism and Machine Theory, vol. 46, 2011. pp. 1601–160.

[4] M. Lawn and T. Ishimatsu, "Modeling of a stair-climbing wheelchair mechanism with high single step capability," IEEE Transactions on Neural Systems and Engineering, vol. 11, no. 3, 2003, pp. 323–332.

[5] Y. Takahashi, S. Ogawa, and S. Machida, "Human assist robot (1st report: Prototype of wheelchair which can fly up and run)," Proc. JSME ROBOMEC'99 1999, Tokyo, pp. 1A1-75-106.

[6] Independence Technology, L.L.C., iBOT, [Online, retrieved: February 2013] http://www.ibotnow.com/, 2008.

[7] K. Taguchi and H. Sato, "A study of the wheel-feet mechanism for stair climbing," Journal of Robotics Society of Japan, vol. 15, 1997, pp. 118–123.

[8] K. Sugiyama, T. Ishimatsu, T. Shigechi, and M. Kurihara, "Development of stair-climbing machines at Nagasaki," Proc. of 3rd International Workshop on Advanced Mechatronics, Berlin, Jun - July 1999, pp. 214–217.

[9] H. Ikeda, Y. Katsumata, M. Shoji, T. Takahashi, and E. Nakano, "Cooperative strategy for a wheelchair and a robot to climb and descend a step," Advanced Robotics, 2008, vol. 22, pp. 1439–1460.

[10] H. Ikeda, H. Kanda, N. Yamashima, and E. Nakano, "Cooperative step-climbing method using a wheelchair and a partner robot," Proceedings of the International Conference on Future Trends in Automation and Robotics - FTAR 2012, Kuala Lumpur, August 2012, pp. 1–6.

 ISBN: 978-1-61208-269-1